Mini review
doi.org/10.1002/elsa.202100156
Chemistry Europe
European Chemical Societies Publishing

Received: 8 September 2021
Revised: 6 October 2021
Accepted: 6 October 2021

Electrochemical generation of nitric oxide for medical applications

Corey J. White | **Nicolai Lehnert** | **Mark E. Meyerhoff**

Department of Chemistry, University of Michigan, Ann Arbor, Michigan, USA

Correspondence
Mark E. Meyerhoff, Department of Chemistry, University of Michigan, 930 North University Avenue, Ann Arbor, MI 48109-1055, USA.
Email: mmeyerho@umich.edu

Funding information
National Institutes of Health, Grant/Award Number: HL132037

Abstract

Over the past 30 years, the significance of nitric oxide (NO) has become increasingly apparent in mammalian physiology. It is biosynthesized by three isoforms of nitric oxide synthases (NOS): neuronal (nNOS), endothelial (eNOS), and inducible (iNOS). nNOS and eNOS both produce low levels of NO (nM) as a signaling agent and vasodilator, respectively. iNOS is present in activated macrophages at sites of infection to generate acutely toxic (μM) levels of NO as part of the mammalian immune defense mechanism. These discoveries have led to numerous animal and clinical studies to evaluate the potential therapeutic utility of NO in various medical operations/treatments, primarily using NO gas (via gas-cylinders) as the NO source. In this review, we focus specifically on recent advances in the electrochemical generation of NO (E-NOgen) as an alternative means to generate NO from cheap and inert sources, and the fabrication and testing of biomedical devices that utilize E-NOgen to controllably generate NO for medical applications.

KEYWORDS
copper catalyst, electrocatalysis, electrochemical nitrite reduction, inhaled nitric oxide, IV-catheters, nitric oxide, silicone-rubber patches

1 | INTRODUCTION

Nitric oxide (NO) is an endogenous gas that plays several key physiological roles in humans, including prevention of platelet activation/adhesion, inhibiting bacterial adhesion and proliferation, enhancing vasodilation, promoting angiogenesis, mediating nerve-signal transduction, and aiding in wound healing.[1–7] At low NO fluxes of 0.5–4.0 $\times$ 10^{-10} mol min^{-1} cm^{-2}, as emitted from a normal-functioning endothelium, NO acts as an anticoagulant, both controlling arteriolar tone and preventing the activation of platelets that approach this surface.[8] NO is also released by macrophages and nasal epithelial cells at higher fluxes, where it acts as a potent antimicrobial agent to combat bacterial infection.[9,10] The antithrombotic and antibacterial properties of NO have resulted in its use to combat clotting and bacterial biofilm formation in several medical applications.

Inhaled nitric oxide (INO) therapy has become a mainstay of intensive care units for lung failure, resulting in preferential pulmonary vasodilation.[11] In cases where neonates have hypoxic respiratory failure, INO has been demonstrated to improve oxygenation and reduce the need for extracorporeal membrane oxygenation therapy.[12,13] Though INO is only approved for hypoxic respiratory failure at present, it has been demonstrated to be beneficial in numerous other treatments, including for pneumonia,[14] acute respiratory distress

Mini review
doi.org/10.1002/elsa.202100156
Chemistry Europe
European Chemical Societies Publishing

syndrome,[15] stroke,[16] cystic fibrosis,[17] tuberculosis,[18] pulmonary hypertension,[19,20] pulmonary fibrosis,[21] chronic obstructive pulmonary disease,[22] and most recently for potential use in treating COVID-19.[23,24] During cardiopulmonary bypass (CPB), NO has also been shown to prevent blood activation (due to the exposure of blood to air),[25] inflammation, and organ failure during heart surgery.[26,27] When NO is added to the sweep gas of an oxygenator during simulated CPB, it has been shown to attenuate blood cell activation.[28–31]

The major limitation to the routine use of NO in emergency rooms and the field is the prohibitively high cost and low portability of current commercial systems for gaseous NO delivery. These require delivering NO via gas cylinders, which are limited to critical care facilities, contain NO at concentrations that can lead to decomposition (due to disproportionation over time) to generate NO_2, a highly toxic gas, and are expensive (~$3000/patient/day).[32] Alternative approaches have been tested to develop more compact/portable NO-delivery systems. For example, a device based on liquid dinitrogen tetroxide (N_2O_4) as a source of NO is under development (GeNO, LLC). N_2O_4 exists in equilibrium with NO_2 (g) that gets passed over a reducing cartridge, ultimately generating NO.[33] The focus of this review is on recent research into alternative, portable, tunable, and low-cost means of generating NO electrochemically from inorganic nitrite ions for medical applications.

2 | BIOMEDICAL APPLICATIONS OF ELECTROCHEMICAL NITRIC OXIDE GENERATION

Taking inspiration from biological copper-nitrite reductases (CuNIR),[34,35] our team has developed a new, low-cost electrochemical method to generate NO from benign precursors for potential use in clinics, ambulances, and in the field. Using CuNIR inorganic model complexes as a starting point, the electrochemical reduction of nitrite (NO_2^-) ions to NO gas can be achieved using specially developed Cu(II)-ligand (Cu(II)-L) complexes as catalysts. Here, the Cu(II)-L complex is initially reduced to the Cu(I)-L form via either an applied current or potential, then binds NO_2^- and rapidly reduces it to NO and water, thereby regenerating the Cu(II)-L form of the catalyst (Figure 1, Equation (1)). Importantly, NO gas levels are tunable depending on the applied voltage or current. The ability to generate NO on-demand from low-cost and stable sources

$$\mathrm{Cu(I)-L} + \mathrm{NO_2^-} + 2\mathrm{H^+} \rightarrow \mathrm{Cu(II)-L} + \mathrm{NO} + \mathrm{H_2O} \quad (1)$$

(e.g., $NaNO_2$) and the ability to tune the concentration of NO generated (applied current/voltage) are both highly desirable in applying this method of NO generation for a variety of biomedical applications. Below we discuss advances in the controlled electrochemical generation of NO (E-NOgen) via this method in three different configurations for three different biomedical applications: intravenous (IV)-catheters, gas-phase NO for INO therapy, and silicone rubber patches for wound healing (Figure 2).

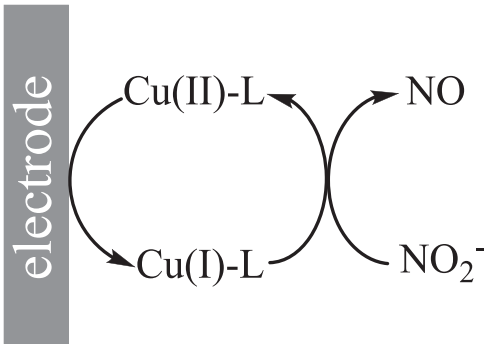

FIGURE 1 Mechanism of electrochemical reduction of NO_2^- to generate NO via a Cu(II)-ligand catalyst

2.1 | IV-catheters

The use of IV-catheters comes with two primary risk factors – thrombus formation and bacterial infection. These risks can range from simple interference with medical care to fatality, with an estimated 28,000 deaths and ~$2.3 billion in additional healthcare costs per year associated with these two complications.[36] Nevertheless, this risk is tolerated because vascular access is essential for diagnoses and treatments. Due to the antithrombotic and antibacterial effects of NO, the generation of NO within catheter devices has been studied extensively in the literature as a potentially novel and convenient solution to mitigate IV-catheter risk factors.[37,38]

A large body of literature details the use of NO donor molecules within polymeric materials, or as coatings on implantable devices, including IV-catheters.[10,39–53] For example, silicone foley catheters impregnated with *S*-nitroso-N-acetylpenicillamine generate surface NO fluxes $> 0.7 \times 10^{-10}$ mol min^{-1} cm^{-2} for over 31 days and result in up to 2.5 log unit decreases in viable *S. epidermis* biofilms at the catheter surface compared to controls.[51] Diazeniumdiolate derivatives (also frequently referred to as NONOates in the literature) have also been studied in catheter/sensor applications. For example, glucose sensors containing a diazeniumdiolated dibutylhexyldiamine coating tested in bovine serum exhibited continuous NO fluxes $> 1.0 \times 10^{-10}$ mol min^{-1} cm^{-2} for 6 days leading to more accurate venous blood glucose

Mini review
doi.org/10.1002/elsa.202100156
Chemistry Europe
European Chemical Societies Publishing

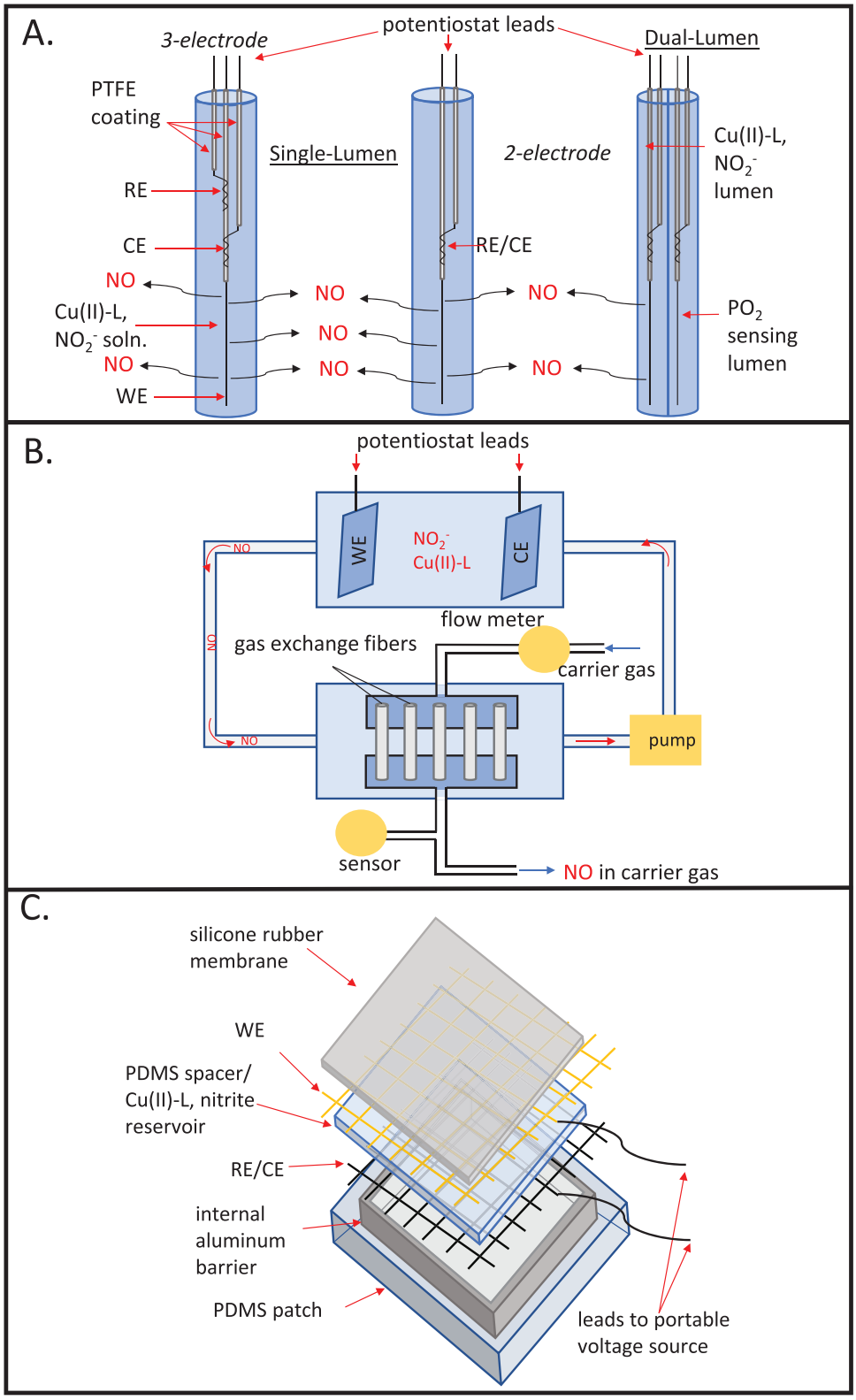

FIGURE 2 Overview of three electrochemical generations of NO (E-NOgen) devices utilized for biomedical applications. **(a)** Two- and three-electrode single-lumen IV-catheters and dual-lumen catheter containing a second PO_2 sensing lumen, **(b)** Bulk NO generator for inhaled NO (INO), and **(c)** NO-releasing silicone rubber patch for wound healing

sensing in rabbit jugular veins compared to controls without the coating.[52] While long-term NO release and anti-thrombotic activity have been demonstrated for several NO donors/coatings, the use of common NO donors such as diazeniumdiolates or *S*-nitrosothiols in NO-releasing catheter devices/coatings is limited by their instability to temperature, photolysis, leaching, and so forth, negatively impacting their storability over time. Furthermore, these NO donor-based methods suffer from low tunability of their NO release profiles – dependent on the nature of the molecule (half-life/kinetics of NO release is molecule/material dependent), and may require rigorous storage and handling conditions to prevent decomposition prior to their use. Consequently, the commercialization of these technologies has been challenging.

Over the past ~10 years, our laboratory has devised and tested a series of copper-based E-NOgen catalysts for use in IV-catheter devices. In our initial report of an E-NOgen-based catheter device, we demonstrated that a single-lumen silicone-rubber catheter containing a Cu^0 working electrode and Ag/AgCl reference/counter electrode with a buffer/nitrite/EDTA solution can generate low concentrations of NO from trace Cu(I) generated at the surface of the Cu^0 electrode under specific conditions.[54] Due to the initial presence of a fouling copper-oxide layer at the surface of the Cu^0 electrode, holding solely at an anodic potential for long periods results in negligible surface oxidation of Cu^0–Cu(I), and correspondingly, negligible NO generation. Instead, a two-step pulse sequence was required, whereby an initial 3-min cathodic potential at –0.7 V (reported versus normal hydrogen electrode (NHE)) was applied to strip the copper-oxide layer, followed by a subsequent 3-min anodic potential at 0.2 V versus NHE to generate Cu(I) at the exposed Cu^0 wire for nitrite reduction. Due to the rapid formation of new copper-oxide layers during the anodic phase, the continued generation of NO from this system required a constant three-minute alternating cathodic/anodic voltage cycle. Low NO fluxes of $0.5–1.0 \times 10^{-10}$ mol min^{-1} cm^{-2} were emitted from the outside surface of the catheter, measured via the gold-standard chemiluminescence NO detection method.[55] Further, in a 7-day antimicrobial study, viable bacterial counts of *E. coli* and *A. baumanni* strains on the outside surface of these NO emitting catheters were reduced by 97% and 98%, respectively. In a subsequent study, the pulse sequence was refined to produce more consistent and increased NO fluxes by reducing the pulse cycle from 3 min to 30 s and by using a –1.3 V applied cathodic potential, respectively.[56] Overall, the limitations of using a Cu^0 working electrode as a source of Cu(I) ions were somewhat prohibitive (requiring sequentially alternating the applied voltage, etc.), but nevertheless, these studies provided preliminary evidence that the preparation of alternative Cu(I)-L catalysts could potentially be employed to electrocatalytically generate pure NO from a NO_2^- source.

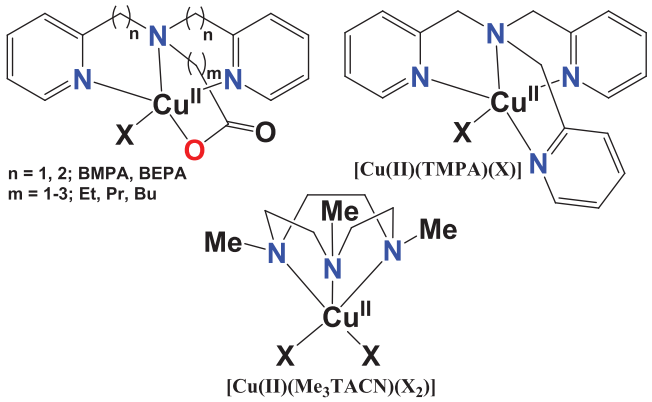

FIGURE 3 Overview of the Cu(II)-ligand (Cu(II)-L) catalysts tested in electrochemical generations of NO (E-NOgen) devices

The next generation of E-NOgen catalysts for IV-catheters took an alternate approach: the design and synthesis of Cu(II)-L catalysts that could be electrocatalytically reduced to the Cu(I)-L state for nitrite reduction (see Figure 1a). This work took inspiration from the type II copper center (T2-Cu) active site of bacterial CuNIRs,[57,58] as well as other reports of Cu(II)/Cu(I) model complexes that can catalyze nitrite reduction chemically/electrochemically.[59–61] In our initial report using this approach, tris(2-pyridylmethyl)amine (TMPA; also commonly abbreviated as TPA or TPMA) was used to generate a Cu(II)-TMPA catalyst (Figure 3a), that exhibits a reversible Cu(II)/Cu(I) couple with E_R = –380 mV versus Ag/AgCl in the absence of nitrite.[62] Single-lumen silicone rubber catheters containing a Pt wire working electrode and an Ag/AgCl reference/counter electrode with the $[Cu(II)(TMPA)]^{2+}$ complex (4 mM in a 0.5 M, pH 7.2 MOPS buffer with 0.2 M NaCl electrolyte and 0.4 M $NaNO_2$) in the bulk solution/reservoir were fabricated. These catheters generated NO fluxes ranging from ~0.5–3.0×10^{-10} mol min^{-1} cm^{-2} and were tunable based on cathodic hold potentials applied to the working Pt electrode (ranging from –0.20 to –0.40 V). Furthermore, continuous NO release at physiologically relevant levels was demonstrated for up to 7 days. In clinical settings, the application of this technology requires the use of dual-lumen catheters (see Figure 2a), whereby one lumen acts as a dedicated E-NOgen compartment while the second lumen is used for clinical purposes (i.e., drug infusion or electrochemical sensing of blood gases, electrolytes, glucose, etc.). As such, both single- and dual-lumen catheters were tested in both in vivo anti-thrombosis trials within a rabbit model, as well as for antimicrobial/biofilm properties using a drip-flow bioreactor (as a model for in vivo conditions). Significant reductions in thrombosis were achieved with both

single and dual lumen catheters after 7 h of NO release compared to controls (83 ± 12% reduction; $p < 0.05$, $n = 3$). Likewise, upon an initial inoculation of *E. coli* on the surface of single- and dual-lumen catheters, followed by a continuous flow of medium containing *E. coli* for 3 days in the bioreactor, a $>10^2$ decrease of viable bacteria was found on the surfaces of the catheters when E-NOgen was turned on for only 3 h per day at a NO flux of 0.6×10^{-10} mol min^{-1} cm^{-2}.

One potential concern with using non-centrosymmetric dual-lumen catheters was whether E-NOgen within one lumen of the catheter could generate adequate NO fluxes at the surface of the other lumen. To address this, a detailed finite element analysis study was performed on single- and dual-lumen catheters, as well as a hypothetical 3-lumen catheter for more centrosymmetric NO release profiles.[63] The transport of NO from the internal E-NOgen lumen to the external surface of a catheter is dictated by NO transport in the bulk E-NOgen medium, as well as through the polymeric catheter material, that is, its partition and diffusion coefficients. Importantly, this study demonstrated that dual-lumen catheters composed of silicone rubber and Elast-Eon 5–325 (silicone polyurethane), both polymers with high NO diffusion and partition coefficients, exhibited asymmetric NO release profiles at 10 min response times, with increasing symmetry in NO release after 20 min. Across the board, polymer materials with higher diffusion coefficients gave faster response times to reach a steady-state and more symmetric NO outer surface fluxes, while the effect of the partition coefficient on response times and symmetry of NO release was more complex. Poor distribution/symmetry of NO was predicted at short response-times (10–20 min) with polymers containing high partition coefficients for NO (likely due to needing higher NO concentrations in the polymer before it is released at the surface of the material), though these ultimately gave the highest NO fluxes at longer response-times (30–40 min). In contrast, rapid and more symmetric distributions of NO at 10–20 min time points were predicted in polymers with lower partition coefficients, ultimately generating lower maximum NO fluxes with longer response times. The results from this study indicated that both silicone rubber and Elast-Eon 5–325 are the best polymer materials to use as IV-catheters for rapid and more symmetric NO release and that within 20–40 min NO is produced at physiologically relevant fluxes at all sides of the catheter.

Our laboratory has also demonstrated that E-NOgen from dual-lumen catheters can in fact enhance the accuracy of electrochemical intravascular sensing of the partial pressure of O_2 (PO_2).[64] Typically, blood analytes are tested periodically in vitro by drawing blood samples, leaving gaps between analyte monitoring that could potentially be detrimental for patient care/diagnostics, especially with critically ill patients. To address this challenge, Ren et al. devised a dual-lumen catheter containing one E-NOgen lumen with a Pt wire working electrode and Ag/AgCl reference/counter electrode containing the Cu(II)-TMPA catalyst in a nitrite/buffer/electrolyte solution (see Figure 2a). The PO_2 sensing lumen consisted of a PFA-coated Pt wire working electrode with an Ag/AgCl wire counter/reference electrode with a 0.1 M bicarbonate buffer at pH 10. The leads from both lumens were connected to separate channels of a multi-channel potentiostat to separately induce E-NOgen by holding the applied potential at –400 mV, and PO_2 sensing by holding the applied potential at –700 mV (both vs. Ag/AgCl) to induce O_2 reduction. In benchtop experiments, the O_2 sensing was fully compatible with E-NOgen – the low NO fluxes produced from E-NOgen do not affect O_2 sensing results relative to controls where the E-NOgen process was not turned on (i.e., the second-order reaction of NO with O_2 is negligible at the concentrations of NO being produced). When tested in vivo within rabbit veins for 7 h and porcine arteries for 21 h, IV-catheters that had E-NOgen turned on were able to continuously measure accurate PO_2 levels over the entire 7 and 21 h duration of the rabbit and porcine experiments, respectively. In contrast, in the controls where E-NOgen was turned off, PO_2 measurements were accurate for only 4 h in rabbit veins and 6 h in porcine arteries before large negative deviations in the sensed PO_2 levels were measured due to the formation of blood clots on the catheter surface (with active platelets in these clots consuming oxygen, lowering the PO_2 levels locally at the surface of the catheters in vivo). This technology could potentially be expanded towards the development of other in vivo sensors for continuous and accurate real-time measurements of different blood analytes to greatly enhance real-time medical diagnostic capabilities.

More recently, we have tested several other Cu(II)-L catalysts to improve catalyst lifetime and NO fluxes (see Figure 3b,c).[65,66] The Cu(II)-Me_3TACN (Me_3TACN = 1,4,7-trimethyl-1,4,7-triazacyclononane) catalyst (Figure 3b) exhibits a reduction potential of ∼–340 mV versus Ag/AgCl. Single- and dual-lumen catheters containing a Pt-wire working electrode and Ag/AgCl wire reference/counter electrode and a solution of 2 mM Cu(II)-Me_3TACN/0.4 M $NaNO_2$/4-(2-hydroxyethyl)-1-piperazineethanesulfonic acid (HEPES) buffer, pH 7.3, within the E-NOgen lumen, were fabricated. These catheters were tested for tunability of NO flux, long-term stability/lifetime, antibacterial properties, and O_2 sensitivity. Notably, NO fluxes were generated with a high degree of tunability – ranging from 0 to 16×10^{-10} mol min^{-1} cm^{-2} (single-lumen) and 0 to 14×10^{-10} mol min^{-1} cm^{-2} (dual-lumen), corresponding to applied

currents of 0 to 20 μA, and from 0 to 17 $\times$ 10^{-10} mol min^{-1} cm^{-2} (single-lumen) and 0 to 15 $\times$ 10^{-10} mol min^{-1} cm^{-2} (dual-lumen) corresponding to applied potentials of 0 to –400 mV versus Ag/AgCl. The Cu(II)-Me_3TACN catalyst produced NO with average Faradaic efficiencies, ranging from 84% at 1 μA applied current to 57% at 11 μA applied current. Furthermore, the continuous release of NO at physiologically useful NO fluxes (at ~5 $\times$ 10^{-10} mol min^{-1} cm^{-2}) was demonstrated for up to 8 days. In antimicrobial studies, dual-lumen catheters with one lumen containing the catalyst (and electrodes) exhibited a greater than the 2 log unit decrease in viable *P. aeruginosa* and slightly under a 3 log unit decrease in viable *S. aureus* cell counts when E-NOgen was only turned on for 6 h per day at a –300 mV hold potential versus Ag/AgCl for 5 days. Despite the significant advances in catalyst lifetime/NO flux/antimicrobial properties compared to previous catalysts, the Cu(II)-Me_3TACN catalyst suffered from two major drawbacks. Owing to its negative reduction potential, this catalyst is O_2 sensitive, and NO fluxes decreased by ~75% when the vessel housing of the catheter was switched from a 100% N_2 sparge gas to a 3% O_2 sparge gas. Additionally, in the presence of low levels of nitrite, CV experiments suggested that disproportionation of the Cu(I) form of the complex to Cu(II) and Cu^0 occurred, the latter of which plated out on the surface of the working electrode over time.

In order to draw detailed comparisons between ligand structure and catalyst properties (i.e. reduction potential, Faradaic efficiencies, turnover frequencies), a series six of Cu(II)-BMPA-/BEPA-/Et/Pr/Bu (BMPA = bis(2-methylpyridyl)amine; BEPA = bis(2-ethylpyridyl)amine) catalysts containing appended carboxylate arms (Et = ethylate, Pr = propionate, and Bu = butylate) were recently studied (Figure 3c).[66] Remarkably, these catalysts span Cu(II)/Cu(I) reduction potentials ranging from –380 mV in Cu(II)-BMPA-Pr to +10 mV for Cu(II)-BEPA-Bu (both vs. Ag/AgCl), whereby the BMPA-carboxylates all exhibit more negative reduction potentials compared to their BEPA-carboxylate analogs. Furthermore, within the series of BMPA-/BEPA-carboxylates, the shorter carboxylate chain lengths correlate with more negative reduction potentials (e.g., BEPA-Et = –250 mV, BEPA-Pr = –80 mV, and BEPA-Bu = 10 mV). Density functional theory (DFT) modeling of this series suggests that the ligand steric constraints affect optimal metal-ligand binding geometries, leading to contracted Cu(II)-pyridine bonds across the BMPA-carboxylate series, causing more negative potentials for the BMPA-carboxylates. Additionally, the optimized BMPA- and BEPA-Et structures had elongated Cu-OOC bond-lengths, leading to further contraction of Cu(II)-pyridine and tertiary amine bonds to compensate for poor donicity from the ethylate arm, which is not long enough to optimally coordinate to the Cu(II) center. With the large range of reduction potentials across the series, several trends were identified in the catalyst properties. For example, the turnover frequencies were directly proportional to the Cu(II)/Cu(I) reduction potential, whereby more reducing catalysts had faster turnover frequencies (BMPA-Et > BMPA-Pr > BMPA-Bu > BEPA-Et > BEPA-Pr > BEPA-Bu), ranging from 11.82/s with Cu(II)-BMPA-Et to 1.18/s with Cu(II)-BEPA-Bu. On the other hand, the Faradaic efficiencies were quite low for BMPA-Et, BMPA-Pr, and BEPA-Et at 15%, 47%, and 23% respectively. The BMPA-Bu, BEPA-Pr, and BEPA-Bu Cu(II) complexes had Faradaic efficiencies of 84%, 94%, and 91%, respectively. These values were ascribed to two competing factors: (1) The more reducing complexes could further reduce/disproportionate generated NO to yield N_2O, and (2) The steric strain in BMPA-/BEPA-Et complexes enhances this disproportionation reaction, leading to deviations in the general trend correlating reduction potential to Faradaic efficiency. The combined data for this series demonstrates that a balance must be struck between reduction potential and catalyst Faradaic efficiency: more positive Cu(II)/Cu(I) couples inhibit the over-reduction of NO to N_2O but such complexes are also slower catalysts.

In catheter studies, Cu(II)-BMPA-Pr was demonstrated to release NO fluxes between 0 – 8 $\times$ 10^{-10} mol min^{-1} cm^{-2} using cathodic hold potentials ranging from 0 to –0.45 V versus Ag/AgCl, and similarly generated NO fluxes between 0–7 $\times$ 10^{-10} mol min^{-1} cm^{-2} using applied currents between 0–15 μA within single-lumen catheters.[65] Cu(II)-BEPA-Pr is the best performing catalyst reported to date, with NO fluxes ranging from 0 – 24 $\times$ 10^{-10} mol min^{-1} cm^{-2} and 0 – 17 $\times$ 10^{-10} mol min^{-1} cm^{-2} in single- and dual-lumen catheter configurations, respectively when applied potentials ranged from 0 to –0.35 V versus Ag/AgCl. In antimicrobial studies with dual-lumen catheters containing the Cu(II)-BEPA-Pr complex, >2 log unit reductions in viable strains of both *P. aeruginosa* and *S. aureus* were reported. Nevertheless, the Cu(II)-BEPA-Pr catalyst suffers from similar O_2 sensitivity problems as Cu(II)-Me_3TACN, with a ~70 % decrease in NO flux when switching from N_2 to 3% O_2 sparge gasses. Even so, the performance and NO fluxes generated from the catalyst were still adequate to achieve significant anti-thrombotic and antimicrobial activities under ambient conditions.

2.2 | INO and cardiopulmonary bypass surgery

The application of our E-NOgen technology using nitrite ions and Cu(II)-L complexes has also been studied and optimized for other potential medical applications

including INO to treat persistent pulmonary hypertension and during CPB surgery.[67] The major risk factor of CPB is white blood cell activation due to the contact of extracorporeal blood with the ambient atmosphere during cardiotomy suction, and a corresponding systemic inflammatory response during the procedure.[68] Recently, our laboratories have sought to test E-NOgen as an alternate and cheaper source of NO (g) for medical procedures like persistent pulmonary hypertension and CBP. Using the E-NOgen principles established for the IV-catheter applications above, a portable gas-phase NO generator was fabricated and tested during CPB with extracorporeal circulation in a porcine model.

The first generation portable E-NOgen device consisted of an 80 ml bulk E-NOgen cell containing 7 mM Cu(II)-Me_3TACN catalyst, 1.0 M $NaNO_2$, and 0.5 M HEPES buffer (pH 7.3), as well as a high-surface-area 50 cm^2 Au-mesh working electrode and 25 cm^2 Pt-mesh counter/reference electrode. In the optimal configuration for NO generation (Figure 2b), the E-NOgen cell solution is circulated rapidly into a gas-extraction cell at flow rates up to 700 ml/min via a micro-liquid pump. A silicone-fiber-based gas exchanger rapidly extracts the highly permeable NO gas from the circulating bulk solution while the remaining solution is recycled back to the pump reservoir and ultimately to the E-NOgen cell to continue generating more NO from the nitrite reservoir. We found that this method of NO (g) extraction was superior to a previously reported configuration using an iron meso-tetrakis(4-N-methylpyridiniumyl)porphyrin as the nitrite reduction catalyst,[69] whereby the NO extraction cell consisted of a bubbler containing the sweep gas with an outlet gas port for the extracted NO plus carrier gas. With the silicone-fiber-based gas exchanger method, upon extraction/transport of NO through the walls of the hollow silicone fibers, a recipient carrier gas (N_2 or air) delivers the NO for potential medical applications. To test the levels of NO being generated in the gas flow, the stream can be monitored continuously with NO/NO_2 selective electrochemical sensors. At a set 0.1 L/min carrier-gas flow rate, output NO levels could be tuned between ~200–400 PPM (with N_2 as the carrier gas) by varying the applied current to the E-NOgen cell from 5–30 μA, with only a 5-min response time between the adjustment of current and generation of steady-state levels of NO. The continuous generation of 400 PPM NO was sustained for up to 24 h. Upon using ambient air as the carrier gas, NO levels decreased by 50%, though NO can still be generated at suitable levels (up to ~180 PPM) for most desired medical applications. The use of ambient air as the carrier gas is ideal, as the device would eliminate the need for any NO and N_2 gas cylinders, greatly enhancing its portability, cost, and utility. However, the reaction of NO with O_2 presents a concern at these higher NO concentrations where the reactivity of NO with O_2 could potentially generate hazardous levels of NO_2. To test NO_2 output levels, an experiment where NO was continuously generated at 60 PPM with air as the carrier gas was conducted. This experiment yielded relatively low concentrations of NO_2 (<1.5 PPM), consistent with the reaction rate of NO in air.[70] The disproportionate decrease in NO output relative to NO_2^- detection suggests that the diminished NO release under increased concentrations of O_2 in the sweep gas is primarily due to the O_2 sensitivity of the Cu(I)-L catalyst and competition between NO_2^- and O_2 binding to the reduced Cu(I)-L center.

The application of this E-NOgen device in CBP was tested in a porcine model where 500 PPM of NO was generated and delivered in a 1:1 N_2:O_2 carrier gas to the blood-oxygenator of a cardiotomy suction unit. CD11B expression in granulocytes and monocytes was monitored as a biomarker for the degree of white blood cell activation. In the experimental group that received 500 PPM of NO, normal values of CD11B in both granulocytes and monocytes were sustained during the 2 h operation, as well as during the subsequent 72 h of post-op monitoring. In contrast, a large increase in CD11B expression was measured in the control group during the procedure (up to 600% relative to the baseline in granulocytes and 250% in monocytes), suggesting an inflammatory response occurred during the operation (termed systemic inflammatory response syndrome). These results provide promising evidence that the E-NOgen technology not only can be utilized specifically for CPB but due to its robust tunability and low cost, could also be further adapted for other medical applications requiring airway delivery of gas-phase NO (i.e., persistent pulmonary hypertension). The device does not require NO gas cylinders (which are expensive and unstable over long time periods) and can generate adequate concentrations of NO using ambient air as a carrier gas source.

2.3 | Wound-healing patches

The antimicrobial properties of NO combined with many of its reported secondary benefits, for example, inhibition of inflammatory responses, increasing angiogenesis, and so forth have led to its testing in NO-based therapeutics for wound-healing applications.[71] This approach is especially useful in cases of chronic wounds and infections, where antimicrobials or antibiotics would typically be utilized over long time periods. With increasing drug-resistant bacterial strains, alternative methods for chronic wound treatment, including NO, have been evaluated. Indeed, several reports utilizing the chemical release of NO have demonstrated that NO-releasing materials such as

nanoparticles and hydrogels can be quite useful in wound-healing applications.[72–75]

We have reported the adaptation of our E-NOgen technology within silicone-rubber patches that can controllably release NO directionally from one surface of the patch (Figure 2c).[76] The device consists of a 10–40 × 10–40 × 5–10 mm patch (several dimensions were fabricated/tested) made from polydimethylsiloxane (PDMS) housing, a cheap and flexible material. Within the housing lies (1) a physical aluminum barrier to force directional NO release at the surface of the patch that adheres to the skin; (2) an Ag/AgCl mesh as the reference/counter electrode; (3) a porous PDMS spacer with an inner chamber housing a 4 mM Cu(II)-TMPA catalyst solution with 0.4 M $NaNO_2$, 0.2 M NaCl, and 0.5 M HEPES (pH 7.2); (4) a gold-sputtered stainless steel mesh working electrode; and (5) an outer surface that would contact the wound site that is sealed with a silicone rubber membrane and adhesive. Since portability is essential for such a device (where the E-NOgen application is not directly involved with ICU medical care), the electrode leads were tested with a portable, battery-powered, voltage supply that can provide potentials within a ±1V range. Across a range of applied potentials between –0.1 and –0.5 V, NO fluxes from 1–8 × 10^{-10} mol min^{-1} cm^{-2} were achieved (patch dimension: 40 × 40 × 6 mm). Additionally, continuous E-NOgen of fluxes between 8–5 × 10^{-10} mol min^{-1} cm^{-2} were sustained over 4 days, and recovery of 8 × 10^{-10} mol min^{-1} cm^{-2} fluxes were demonstrated upon replacement of the internal catalyst solution with a fresh nitrite/Cu(II)-TMPA stock solution after 4 days. In antimicrobial studies with the E-NOgen patches placed on blood agar plates, viable *E. coli* counts were reduced by 35% after 6 h of E-NOgen, 2 log units after 24 h of E-NOgen, and 3 log units after 48 h of E-NOgen (all with respect to control patches where E-NOgen was not powered on to provide NO). Similarly, viable *S. aureus* decreased by 20% after 6 h and 3 log units after 24 h of continuous E-NOgen. These results demonstrate that low-cost PDMS patches with mesh electrodes in contact with a solution of nitrite and Cu(II)-L complex can serve as an inexpensive and effective means of controllably inhibiting the proliferation of infectious bacteria at sites of chronic infection.

3 | CONCLUSIONS

The beneficial biomedical properties of NO have been investigated for some time. A large body of research to date has focused on the use of gaseous NO or NO-donor molecules (i.e., *S*-nitrosothiols or diazeniumdiolates) to deliver NO for vasodilation, antimicrobial, and anti-thrombotic purposes. Indeed, INO is already approved for treating pulmonary hypertension in newborn babies and adults. Gas-phase NO has also been used off-label in certain medical applications (CBP, see above) and shown to be beneficial in numerous others, but present technologies for NO administration are limited to emergency rooms/hospital settings due to portability and cost constraints. The recent advances in the design and testing of new biomedical devices that carry out E-NOgen highlight a potential means of making NO treatments much more cost-efficient by using cheap/inert $NaNO_2$ as an NO reservoir, and more portable by the design of compact electrochemical devices and portable voltage sources. For the devices discussed herein, one major limitation to the overall catalyst lifetime and concentration of NO generated is the O_2 sensitivity of the Cu(II)-L catalysts in their reduced form. The continued tuning of the Cu(II)/Cu(I) reduction potentials via synthesis of new Cu(II)-L catalysts may provide a means to reduce or eliminate O_2 sensitivity, allowing for significant elongation of catalyst lifetimes. At even more positive Cu(II)/Cu(I) potentials than those reported for our BMPA-/BEPA-carboxylate ligand series,[65,66] over-reduction of NO to N_2O would certainly be mitigated, but a new balance between minimizing/eliminating catalyst O_2 sensitivities and the decreasing turnover frequencies of such catalysts will need to be struck. For IV-catheter applications, catalysts that can tolerate up to 11%–15% O_2 (for use in more O_2-rich arteries) while still generating NO fluxes of 1–4 × 10^{-10} mol min^{-1} cm^{-2} are desirable, while for CBP, INO, and wound-healing patches, O_2 tolerance of up to 20% or greater would be ideal. For CBP/INO, this would allow for ambient air to be used as the carrier gas. Since the wound-healing patch design has no way to sparge or eliminate atmospheric O_2 levels in the Cu(II)-L/NO_2^- reservoir, tolerance to ambient O_2 levels would be even more desirable. Further catalyst development in this direction is in progress. Additionally, for NO-generating technologies to be used for medical purposes, the tight control of output NO levels is essential for their use in the field. While the Cu(II)-L catalysts discussed herein can generate a wide range of NO fluxes by tuning either the applied potential or current, the bulk catalyst solution slowly becomes more basic. This leads to a slow decrease in catalyst activity, and correspondingly, lower NO fluxes overtime when holding at either a constant current or potential. The incorporation and optimization of feedback controls to allow for precise NO monitoring and automated adjustment of the applied currents/voltages to achieve consistent levels of NO generation would greatly benefit the development of these technologies for ultimate use in the medical field.

The physiological functions of NO and the potential for corresponding biomedical applications are numerous and extend beyond the anti-thrombotic, antimicrobial, and anti-inflammatory emphasis of this review. For example,

one recent publication reports the design of an implantable E-NOgen device that utilizes Fe_3S_4 nanoparticles containing a surface Pt-dopant to reduce a $NaNO_2$ source to NO.[77] Here, the device was implanted into a mouse brain and the effect of controlled electrochemical-mediated NO release on NO-dependent neuronal signaling was visualized. We expect that the continued optimization of cost, portability, tunability, and stability/lifetime of the catalysts will be essential in the advancement of existing and newer E-NOgen-based biomedical devices for applications in clinics at scale.

ACKNOWLEDGMENT

The authors acknowledge funding from the National Institute of Health (HL132037).

CONFLICT OF INTEREST

The authors declare no conflict of interest.

DATA AVAILABILITY STATEMENT

Not applicable.

ORCID

Mark E. Meyerhoff https://orcid.org/0000-0002-7841-281X

REFERENCES

1. B. T. Mellion, L. J. Ignarro, E. H. Ohlstein, E. G. Pontecorvo, A. L. Hyman, P. J. Kadowitz, *Blood* **1981**, *57*, 946.
2. M. W. Radomski, R. M. Palmer, S. Moncada, *Br. J. Pharmacol.* **1987**, *92*, 181.
3. S. Moncada, R. M. Palmer, E. A. Higgs, *Pharmacol. Rev.* **1991**, *43*, 109–142.
4. F. C. Fang, *J. Clin. Invest.* **1997**, *99*, 2818–2825.
5. A. Chaux, X. M. Ruan, M. C. Fishbein, Y. Ouyang, S. Kaul, J. A. Pass, J. M. Matloff, *J. Thorac. Cardiovasc. Surg.* **1998**, *115*, 604–614.
6. J. D. Luo, A. F. Chen, *Acta Pharmacol. Sin.* **2005**, *26*, 259–264.
7. J. P. Wallis, *Transfus. Med.* **2005**, *15*, 1–11.
8. M. W. Vaughn, L. Kuo, J. C. Liao, *Am. J. Physiol.* **1998**, *274*, H2163-2176.
9. J. J. Rouby, *Am. J. Respir. Crit Care Med.* **2003**, *168*, 265–266.
10. M. H. Genevieve, K. M. Pradip, *Anti-Infect. Agents Med. Chem.* **2010**, *9*, 187–197.
11. B. C. Creagh-Brown, M. J. D. Griffiths, T. W. Evans, *Crit. Care.* **2009**, *13*, 221-221.
12. Neonatal Inhaled Nitric Oxide Study Group. *N. Engl. J. Med.* **1997**, *336*, 597–604.
13. J. D. Roberts, J. R. Fineman, F. C. Morin, P. W. Shaul, S. Rimar, M. D. Schreiber, R. A. Polin, M. S. Zwass, M. M. Zayek, I. Gross, M. A. Heymann, W. M. Zapol, K. G. Thusu, T. M. Zellers, M. E. Wylam, A. Zaslavsky, *N. Engl. J. Med.* **1997**, *336*, 605–610.
14. H. Blomqvist, C. J. Wickerts, M. Andreen, U. Ullberg, A. Ortqvist, C. Frostell, *Acta Anaesthesiol. Scand.* **1993**, *37*, 110–114.
15. R. P. Dellinger, S. W. Trzeciak, G. J. Criner, J. L. Zimmerman, R. W. Taylor, H. Usansky, J. Young, B. Goldstein, *Crit. Care.* **2012**, *16*, R36.
16. C. Charriaut-Marlangue, P. Bonnin, A. Gharib, P. L. Leger, S. Villapol, M. Pocard, P. Gressens, S. Renolleau, O. Baud, *Stroke* **2012**, *43*, 3078–3084.
17. F. Ratjen, S. Gärtig, H. G. Wiesemann, H. Grasemann, *Respir. Med.* **1999**, *93*, 579–583.
18. R. Long, R. Jones, J. Talbot, I. Mayers, J. Barrie, M. Hoskinson, B. Light, *Antimicrob. Agents Chemother.* **2005**, *49*, 1209–1212.
19. R. N. Channick, J. W. Newhart, F. W. Johnson, P. J. Williams, W. R. Auger, P. F. Fedullo, K. M. Moser, *Chest* **1996**, *109*, 1545–1549.
20. G. M. Pérez-Peñate, G. Juliá-Serdà, N. Ojeda-Betancort, A. García-Quintana, J. Pulido-Duque, A. Rodríguez-Pérez, P. Cabrera-Navarro, M. A. Gómez-Sánchez, *J. Heart Lung Transpl.* **2008**, *27*, 1326–1332.
21. G. L. Yung, J. M. Kriett, S. W. Jamieson, F. W. Johnson, J. Newhart, K. Kinninger, R. N. Channick, *J. Heart Lung Transpl.* **2001**, *20*, 1224–1227.
22. K. Vonbank, R. Ziesche, T. W. Higenbottam, L. Stiebellehner, V. Petkov, P. Schenk, P. Germann, L. H. Block, *Thorax* **2003**, *58*, 289–293.
23. C. Lotz, R. M. Muellenbach, P. Meybohm, H. Mutlak, P. M. Lepper, C. B. Rolfes, A. Peivandi, J. Stumpner, M. Kredel, P. Kranke, I. Torje, C. Reyher, *Acta. Anaesthesiol. Scand.* **2021**, *65*, 629–632.
24. R. Parikh, C. Wilson, J. Weinberg, D. Gavin, J. Murphy, C. C. Reardon, *Ther. Adv. Respir. Dis.* **2020**, *14*, 175346662093351.
25. A. M. El-Sabbagh, C. J. Toomasian, J. M. Toomasian, G. Ulysse, T. Major, R. H. Bartlett, *ASAIO J.* **2013**, *59*, 474–479.
26. J. G. Laffey, J. F. Boylan, D. C. Cheng, *Anesthesiology* **2002**, *97*, 215–252.
27. S. Salis, V. V. Mazzanti, G. Merli, L. Salvi, C. C. Tedesco, F. Veglia, E. Sisillo, *J. Cardiothorac. Vasc. Anesth.* **2008**, *22*, 814–822.
28. M. Chello, P. Mastroroberto, A. R. Marchese, G. Maltese, E. Santangelo, B. Amantea, *Anesthesiology* **1998**, *89*, 443–448.
29. K. Mellgren, L. G. Friberg, G. Mellgren, T. Hedner, A. Wennmalm, H. Wadenvik, *Ann. Thorac. Surg.* **1996**, *61*, 1194–1198.
30. P. A. Checchia, R. A. Bronicki, J. T. Muenzer, D. Dixon, S. Raithel, S. K. Gandhi, C. B. Huddleston, *J. Thorac. Cardiovasc. Surg.* **2013**, *146*, 530–536.
31. C. James, J. Millar, S. Horton, C. Brizard, C. Molesworth, W. Butt, *Intensive Care Med.* **2016**, *42*, 1744–1752.
32. F. S. Cole, C. Alleyne, J. D. Barks, R. J. Boyle, J. L. Carroll, D. Dokken, W. H. Edwards, M. Georgieff, K. Gregory, M. V. Johnston, M. Kramer, C. Mitchell, J. Neu, D. M. Pursley, W. M. Robinson, D. H. Rowitch, *Pediatrics* **2011**, *127*, 363–369.
33. Q. Shen, K. Hedberg, *J. Phys. Chem. A* **1998**, *102*, 6470–6476.
34. A. C. Merkle, N. Lehnert, *Dalton Trans.* **2012**, *41*, 3355–3368.
35. S. Horrell, D. Kekilli, R. W. Strange, M. A. Hough, *Metallomics* **2017**, *9*, 1470–1482.
36. N. P. O'Grady, M. Alexander, E. P. Dellinger, J. L. Gerberding, S. O. Heard, D. G. Maki, H. Masur, R. D. McCormick, L. A. Mermel, M. L. Pearson, I. I. Raad, A. Randolph, R. A. Weinstein, *Morbidity Mortality Wkly. Rep.* **2002**, *51*, 1–26.
37. Y. Wo, E. J. Brisbois, R. H. Bartlett, M. E. Meyerhoff, *Biomater. Sci.* **2016**, *4*, 1161–1183.
38. V. N. Varu, N. D. Tsihlis, M. R. Kibbe, *Vasc. Endovasc. Surg.* **2009**, *43*, 121–131.

39. M. H. Schoenfisch, K. A. Mowery, M. V. Rader, N. Baliga, J. A. Wahr, M. E. Meyerhoff, *Anal. Chem.* **2000**, *72*, 1119–1126.
40. H. Zhang, G. M. Annich, J. Miskulin, K. Osterholzer, S. I. Merz, R. H. Bartlett, M. E. Meyerhoff, *Biomaterials.* **2002**, *23*, 1485–1494.
41. P. N. Coneski, M. H. Schoenfisch, *Polym. Chem.* **2011**, *2*, 906–913.
42. P. G. Parzuchowski, M. C. Frost, M. E. Meyerhoff, *J. Am. Chem. Soc.* **2002**, *124*, 12182–12191.
43. J. M. Buergler, F. O. Tio, D. G. Schulz, M. M. Khan, W. Mazur, B. A. French, A. E. Raizner, N. M. Ali, *Coron. Artery Dis.* **2000**, *11*, 351–357.
44. H. Zhang, G. M. Annich, J. Miskulin, K. Stankiewicz, K. Osterholzer, S. I. Merz, R. H. Bartlett, M. E. Meyerhoff, *J. Am. Chem. Soc.* **2003**, *125*, 5015–5024.
45. M. M. Reynolds, J. A. Hrabie, B. K. Oh, J. K. Politis, M. L. Citro, L. K. Keefer, M. E. Meyerhoff, *Biomacromolecules* **2006**, *7*, 987–994.
46. Y. Wu, A. P. Rojas, G. W. Griffith, A. M. Skrzypchak, N. Lafayette, R. H. Bartlett, M. E. Meyerhoff, *Sens. Actuators B Chem.* **2007**, *121*, 36–46.
47. T. C. Major, D. O. Brant, C. P. Burney, K. A. Amoako, G. M. Annich, M. E. Meyerhoff, H. Handa, R. H. Bartlett, *Biomaterials* **2011**, *32*, 5957–5969.
48. M. C. Jen, M. C. Serrano, R. van Lith, G. A. Ameer, *Adv. Funct. Mater.* **2012**, *22*, 239–260.
49. H. Handa, E. J. Brisbois, T. C. Major, L. Refahiyat, K. A. Amoako, G. M. Annich, R. H. Bartlett, M. E. Meyerhoff, *J. Mater. Chem. B.* **2013**, *1*, 3578–3587.
50. H. Handa, T. C. Major, E. J. Brisbois, K. A. Amoako, M. E. Meyerhoff, R. H. Bartlett, *J. Mater. Chem. B.* **2014**, *2*, 1059–1067.
51. A. Colletta, J. Wu, Y. Wo, M. Kappler, H. Chen, C. Xi, M. E. Meyerhoff, *ACS Biomater. Sci. Eng.* **2015**, *1*, 416–424.
52. A. K. Wolf, Y. Qin, T. C. Major, M. E. Meyerhoff, *Chin. Chem. Lett.* **2015**, *26*, 464–468.
53. A. R. Ketchum, M. P. Kappler, J. Wu, C. Xi, M. E. Meyerhoff, *J. Mater. Chem. B.* **2016**, *4*, 422–430.
54. L. Höfler, D. Koley, J. Wu, C. Xi, M. E. Meyerhoff, *RSC Adv.* **2012**, *2*, 6765–6767.
55. P. N. Coneski, M. H. Schoenfisch, *Chem. Soc. Rev.* **2012**, *41*, 3753–3758.
56. H. Ren, A. Colletta, D. Koley, J. Wu, C. Xi, T. C. Major, R. H. Bartlett, M. E. Meyerhoff, *Bioelectrochemistry* **2015**, *104*, 10–16.
57. M. Kukimoto, M. Nishiyama, M. E. P. Murphy, S. Turley, E. T. Adman, S. Horinouchi, T. Beppu, *Biochemistry* **1994**, *33*, 5246–5252.
58. E. T. Adman, J. W. Godden, S. Turley, *J. Biol. Chem.* **1995**, *270*, 27458–27474.
59. S. C. N. Hsu, Y. - L. Chang, W. - J. Chuang, H. - Y. Chen, I. J. Lin, M. Y. Chiang, C. - L. Kao, H. - Y. Chen, *Inorg. Chem.* **2012**, *51*, 9297–9308.
60. M. Kumar, N. A. Dixon, A. C. Merkle, M. Zeller, N. Lehnert, E. T. Papish, *Inorg. Chem.* **2012**, *51*, 7004–7006.
61. Y. - L. Chang, Y. - F. Lin, W. - J. Chuang, C. - L. Kao, M. Narwane, H. - Y. Chen, M. Y. Chiang, S. C. N. Hsu, *Dalton Trans.* **2018**, *47*, 5335–5341.
62. H. Ren, J. Wu, C. Xi, N. Lehnert, T. Major, R. H. Bartlett, M. E. Meyerhoff, *ACS Appl. Mater. Interfaces.* **2014**, *6*, 3779–3783.
63. H. Ren, J. L. Bull, M. E. Meyerhoff, *ACS Biomater. Sci. Eng.* **2016**, *2*, 1483–1492.
64. H. Ren, M. A. Coughlin, T. C. Major, S. Aiello, A. Rojas Pena, R. H. Bartlett, M. E. Meyerhoff, *Anal. Chem.* **2015**, *87*, 8067–8072.
65. K. K. Konopińska, N. J. Schmidt, A. P. Hunt, N. Lehnert, J. Wu, C. Xi, M. E. Meyerhoff, *ACS Appl. Mater. Interfaces.* **2018**, *10*, 25047–25055.
66. A. P. Hunt, A. E. Batka, M. Hosseinzadeh, J. D. Gregory, H. K. Haque, H. Ren, M. E. Meyerhoff, N. Lehnert, *ACS Catal.* **2019**, *9*, 7746–7758.
67. Y. Qin, J. Zajda, E. J. Brisbois, H. Ren, J. M. Toomasian, T. C. Major, A. Rojas-Pena, B. Carr, T. Johnson, J. W. Haft, R. H. Bartlett, A. P. Hunt, N. Lehnert, M. E. Meyerhoff, *Mol. Pharmaceutics.* **2017**, *14*, 3762–3771.
68. K. Lau, H. Shah, A. Kelleher, N. Moat, *J. Cardiothorac. Surg.* **2007**, *2*, 46.
69. Y. Chi, J. Chen, K. Aoki, *Inorg. Chem.* **2004**, *43*, 8437–8446.
70. U. Schedin, C. G. Frostell, L. E. Gustafsson, *Br. J. Anaesth.* **1999**, *82*, 182–192.
71. A. W. Carpenter, M. H. Schoenfisch, *Chem. Soc. Rev.* **2012**, *41*, 3742–3752.
72. A. R. Bokhari, G. A. Murrell, *J. Shoulder Elbow Surg.* **2012**, *21*, 238–244.
73. M. Champeau, V. Póvoa, L. Militão, F. M. Cabrini, G. F. Picheth, F. Meneau, C. P. Jara, E. P. de Araujo, M. G. de Oliveira, *Acta Biomater.* **2018**, *74*, 312–325.
74. M. I. Santos, L. C. E. da Silva, M. P. Bomediano, D. M. Catori, M. C. Gonçalves, M. G. de Oliveira, *Soft Matter.* **2021**, *17*, 6352–6361.
75. C. Yang, H. H. Hwang, S. Jeong, D. Seo, Y. Jeong, D. Y. Lee, K. Lee, *Int. J. Nanomed.* **2018**, *13*, 6517–6530.
76. W. H. Lee, H. Ren, J. Wu, O. Novak, R. B. Brown, C. Xi, M. E. Meyerhoff, *ACS Biomater. Sci. Eng.* **2016**, *2*, 1432–1435.
77. J. Park, K. Jin, A. Sahasrabudhe, P. - H. Chiang, J. H. Maalouf, F. Koehler, D. Rosenfeld, S. Rao, T. Tanaka, T. Khudiyev, Z. J. Schiffer, Y. Fink, O. Yizhar, K. Manthiram, P. Anikeeva, *Nat. Nanotechnol.* **2020**, *15*, 690–697.

How to cite this article: C. J. White, N. Lehnert, M. E. Meyerhoff, *Electrochem Sci Adv*. **2022**, *2*, e2100156. https://doi.org/10.1002/elsa.202100156